ACCOUNTS
of chemical research

Multifunctional Compact Hybrid Au Nanoshells: A New Generation of Nanoplasmonic Probes for Biosensing, Imaging, and Controlled Release

YONGDONG JIN*

State Key Laboratory of Electroanalytical Chemistry, Changchun Institute of Applied Chemistry, Chinese Academy of Sciences, Changchun 130022, Jilin, P. R. China

RECEIVED ON APRIL 7, 2013

CONSPECTUS

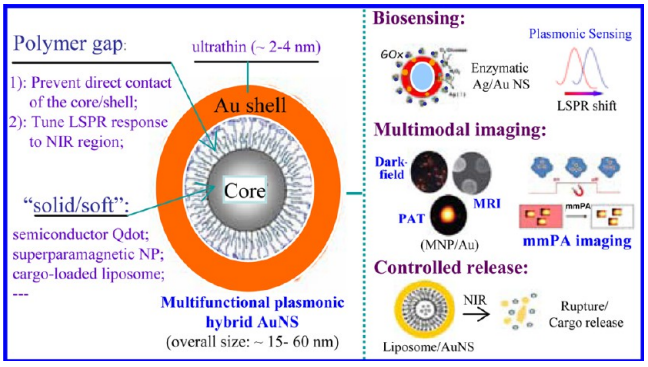

Gold nanoshells (AuNSs) with tunable localized surface plasmon resonance (LSPR) peaks in the near-infrared (NIR) region possess unique optical properties—particularly that soft tissues are "transparent" at these wavelengths—making them of great interest in cancer diagnosis and treatment. Since 1998 when Halas and co-workers invented the first generation of AuNS, with a silica core and Au shell, researchers have studied and designed AuNSs for theranostic—individualized, combination diagnosis and therapy—nanomedicine. As demand has increased for more powerful and practical theranostic applications, so has demand for the next generation of AuNSs—compact yet complex multifunctional AuNSs with finely integrated plasmonic and nonplasmonic inorganic components.

For in vivo biomedical applications, such a hybrid AuNS offers the desirable optical properties of NIR LSPR. Size, however, has proved a more challenging parameter to control in hybrid AuNSs. The ideal size of therapeutic NPs is 10−100 nm. Larger particles have limited diffusion in the extracellular space, while particles less than 5 nm are rapidly cleared from the circulation through extravasation or renal clearance. Conventional methods of preparing AuNS have failed to obtain small-sized hybrid AuNSs with NIR LSPR responses.

In this Account, we present a new class of multifunctional hybrid AuNSs with ultrathin AuNSs and varied, functional (nonplasmonic) core components ranging from "hard" semiconductor quantum dots (QDs), to superparamagnetic NPs, to "soft" liposomes made using poly-L-histidine as a template to direct Au deposition. The resultant hybrid AuNSs are uniform and compact (typically 15−60 nm) but also preserve the optical properties and shell-type NIR response necessary for biomedical use. We also demonstrate these particles' innovative plasmonic applications in biosensing, multimodal imaging and controlled release. More importantly, the magnetic-plasmonic Fe_3O_4/Au core−shell NP enables a new biological imaging method—magnetomotive photoacoustic (mmPA) imaging, which suppresses the nonmagnetomotive background and therefore offers remarkable contrast enhancement and improved specificity compared with photoacoustic images using conventional NP contrast agents.

The advantages of our AuNSs are obvious: they are monodisperse, small (<100 nm), highly integrated, and have tunable visible-NIR plasmonic responses. All of these properties are crucial for in vitro or in vivo biological/biomedical studies and many applications, especially for studies of single cells or molecules which require particle monodispersity and tight size control. The plasmonic fluorescent QD/Au and the magnetic plasmonic Fe_3O_4/Au core−shell NPs may also reveal new physical phenomena that may lead to useful applications, owing to their well-defined core−shell nanoarchitectures and underlying nanoscale physical interactions.

Introduction

In the past decade, noble metal nanoparticles (NPs) have sparked wide interest due to the unique optical properties related to their localized surface plasmon resonance (LSPR) and have led to a variety of research fields ranging from ultrasensitive biosensing and imaging,[1−3] nanomedicine,[4]

Published on the Web 08/30/2013 www.pubs.acs.org/accounts
10.1021/ar400086e

nanophotonics,[5] to plasmonic solar cells.[6] Gold nanoshells (AuNSs), representing one important class of nanostructures with tunable LSPR peaks in the near-infrared (NIR) region (from 700 to 900 nm), the transparent window of soft tissues desired for in vivo applications, have garnered considerable attention in recent years for cancer theranostic applications.[7] The first generation of AuNSs, a silica core/Au shell NP, was invented by Halas et al.[8] in 1998 and further exploited by the authors for innovative photothermal cancer therapy in 2003.[7] Nowadays, such class of NSs has been widely used as a versatile, multifaceted platform for a variety of biomedical applications. With the increased demand for more powerful and practical theranostic applications, the next generation of theranostic AuNSs is highly desired and envisioned to be more complex multifunctional AuNSs with nanometer-scale finely integrated plasmonic and nonplasmonic inorganic components.

Combining multiple discrete components, such as semiconductor quantum dots (QDs), magnetic NPs (MNPs), and plasmonic AuNPs, into a single and compact NP has been proved useful in a variety of applications. Such kind of multimodality imaging nanoprobes have an advantage over single-modality ones since the complementary ability of different imaging modalities could be harnessed to great effect by using them in tandem[9] to circumvent the disadvantage and limitation of each single imaging modality. It will therefore have profound impact on molecular diagnostics, imaging, and therapeutics. For biomedical applications, the ideal sizes of therapeutic NPs should be in the range of 10−100 nm, as larger particles have limited diffusion in the extracellular space,[10] while particles <5 nm are rapidly cleared from the circulation through extravasation or renal clearance.[11] Although a spherical NP with core−shell architecture is an elegant and compact way to combine multiple functionalities of the core and shell materials on nanoscale, practical preparations often result in large particles with overall size > 100 nm and uneven surfaces,[12] and therefore, it still remains a great challenge.

Recently, Jin, Gao, and co-workers[13−15] have devised innovative syntheses of hybrid core−shell NPs with ultrathin plasmonic AuNSs and varied functional (nonplasmonic) core components ranging from "hard" semiconductor QD,[13] MNP,[14] to "soft" liposomes,[15] by using poly-L-histidine (PLH) as template to direct controlled Au deposition. The resultant hybrid AuNSs were monodispersed and compact in sizes (typically 15−60 nm). By creating a few-nanometers scale polymer layers (as a dielectric gap) between the semiconductor[13] or metal oxide[14] core and metallic Au shell, we succeeded in solving fluorescence quenching problem of the QD/Au core−shell NPs[13] and tuning effectively LSPR response of the small sized (<40 nm) Fe_3O_4/Au core−shell NPs (from visible) into the NIR region,[14] which is desirable for potential in vivo bioapplications. More importantly, the resultant magnetic-plasmonic Fe_3O_4/Au NP enables a new biological imaging method, magnetomotive photoacoustic (mmPA) imaging modality.[14] Such kind of compact hybrid core−shell NPs represents a next generation of multifunctional AuNSs and will be gradually attracting extensive attention for biological/biomedical applications.

In this Account, we first summarize our efforts toward the design and wet-chemical synthesis of multifunctional compact hybrid AuNSs, including plasmonic-fluorescent QD/Au, magnetic-plasmonic Fe_3O_4/Au core−shell NPs, liposomal AuNS nanocontainers, and enzyme-responsive Ag/Au bimetallic NSs, with emphasis on the wet-chemical synthetic strategies and their unique multifunctional plasmonic properties. We then highlight their innovative plasmonic applications in biosensing, multimodality imaging, and controlled cargo release applications. Finally, some perspectives in the field are briefly proposed.

Synthesis

QD/Au Core−Shell NPs. Individually, fluorescent QDs[16] and plasmonic AuNSs[7] are both promising and have been recently widely used for a variety of biological/biomedical applications. Combining such two components into a single core−shell NP is, however, a long-standing barrier since the signature optical property of the QDs, fluorescence, will be nearly completely quenched by direct contact with Au in the core−shell format. On the other hand, traditional methods for AuNS formation are failed to produce compact core−shell NPs with smooth and ultrathin AuNSs because of the large size of the Au nuclei.[8]

We solved these problems by developing a biomimetic approach of AuNS formation by using PLH as templates to direct Au nucleation and growth.[13] In contrast to the commonly used primary amines,[8] an important feature of PLH is that its histidine groups are capable of immobilizing Au^{3+} ions at very high packing density for desirable deposition of thin-and-smooth AuNSs. As schematically shown in Figure 1a, hydrophobic CdSe/ZnS QDs coated with trioctylphosphine oxide (TOPO) were first solubilized with an amphiphilic lipid-PEG-COOH conjugate. The water-soluble QDs were then coated with PLH for immobilization of Au^{3+} ions. The compact organic ligand and amphiphilic lipid monolayers serving as an effective barrier against Au direct

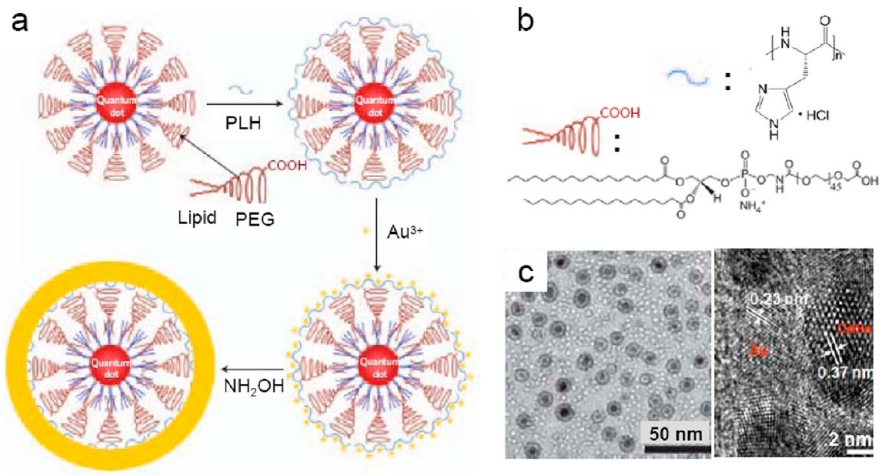

FIGURE 1. (a) Schematic of Au-shell-encapsulated QDs. Hydrophobic TOPO-coated QDs (TOPO, blue) were solubilized with a lipid-PEG-COOH conjugate (purple). The water-soluble QDs were then coated with PLH (blue) for immobilization of Au^{3+} ions. Hydroxylamine was used for Au nucleation on the PLH template and formation of a thin AuNS. (b) The molecular structures of lipid-PEG-COOH and PLH. (c) TEM and HRTEM images of the as-prepared QD/Au core–shell NPs. Reprinted with permission from ref 13. Copyright 2009 NPG.

contact with QDs is crucial to maintain fluorescence of the QDs. After incubation with suitable amount of Au^{3+} for a few minutes, a mild reducing agent, hydroxylamine hydrochloride ($NH_2OH \cdot HCl$), was added to the purified QD-PLH solution, leading to Au nucleation on the PLH template and formation of a thin AuNS. Because $HAuCl_4$ is highly acidic, the pH value of the reaction solution was adjusted to 9–10 with NaOH before the reaction to avoid QD damage. Figure 1c shows representative TEM and high resolution TEM (HRTEM) images of the as-prepared QD/Au NPs, with overall sizes of 15–20 nm, a transparent polymer gap of ~3 nm, and AuNS thickness of ~2–3 nm. The separation between the QD core and Au shell is determined by the size of the polyethylene glycol (PEG) chains and can be increased with nanometer precision by adding, for example, alternating polyelectrolyte monolayers such as polyallylamine hydrochloride (PAH, cationic) and sodium polystyrene sulfonate (PSS, anionic).[13] We noted that mechanical stirring/or vortexing manipulation during the reaction process is crucial to uniform formation of AuNSs, otherwise (if leave the reaction statically) QD/Au core–satellite NPs will dominate the product.

Fe_3O_4/Au Core–Shell NPs. Superparamagnetic Fe_3O_4 NP, an important contrast agent in T_2-weighted magnetic resonance imaging (MRI), represents another type of next generation NPs with particular promise as theranostic agents for clinical applications. The integration of magnetic and plasmonic functions into a compact core–shell NP therefore has obvious benefits for biomedical applications. In addition, with Au coating, the magnetic NPs can be stabilized more efficiently in corrosive biological conditions and readily functionalized through the well-developed Au–S chemistry.

Direct coating of MNPs with Au, however, is a difficult task due to the dissimilar nature of the two surfaces. Usually, direct deposition of Au on MNP surface, by iterative hydroxylamine seeding[17] or by reducing $HAuCl_4$ in a chloroform solution of oleylamine,[18] results in either poor shell morphology or failed in producing small-sized NPs with NIR response. A common way to make NIR-responsive Fe_3O_4/Au hybrid or core–shell NPs is still reliant upon the modified seed-mediated growth approach, resulting in large NPs of 100–200 nm in diameter with uneven surfaces.[12,14] Typically small-sized AuNP seeds are first attached to the surface of amino-modified silica (or polystyrene) nano/microspheres and then allowed to grow to form a shell. Figure 2 (top) shows the synthetic approach of an example, and corresponding TEM images of the products obtained after each synthetic step.

To produce monodisperse Fe_3O_4/Au core–shell NPs with NIR response (critical for in vivo imaging and therapy) and yet maintain compact particle size, we used an approach similar to the preparation of QD/Au core–shell NPs.[14] As schematically shown in Figure 2a (bottom), highly uniform Fe_3O_4 NPs with hydrophobic surface ligands, oleic acid, are first solubilized into an aqueous solution using phospholipid-polyethylene glycol terminated with carboxylic acid (PL-PEG-COOH). The hydrophobic PL segment interdigitates with oleic acids through hydrophobic interactions, whereas the PEG block facing outward renders MNPs water-soluble

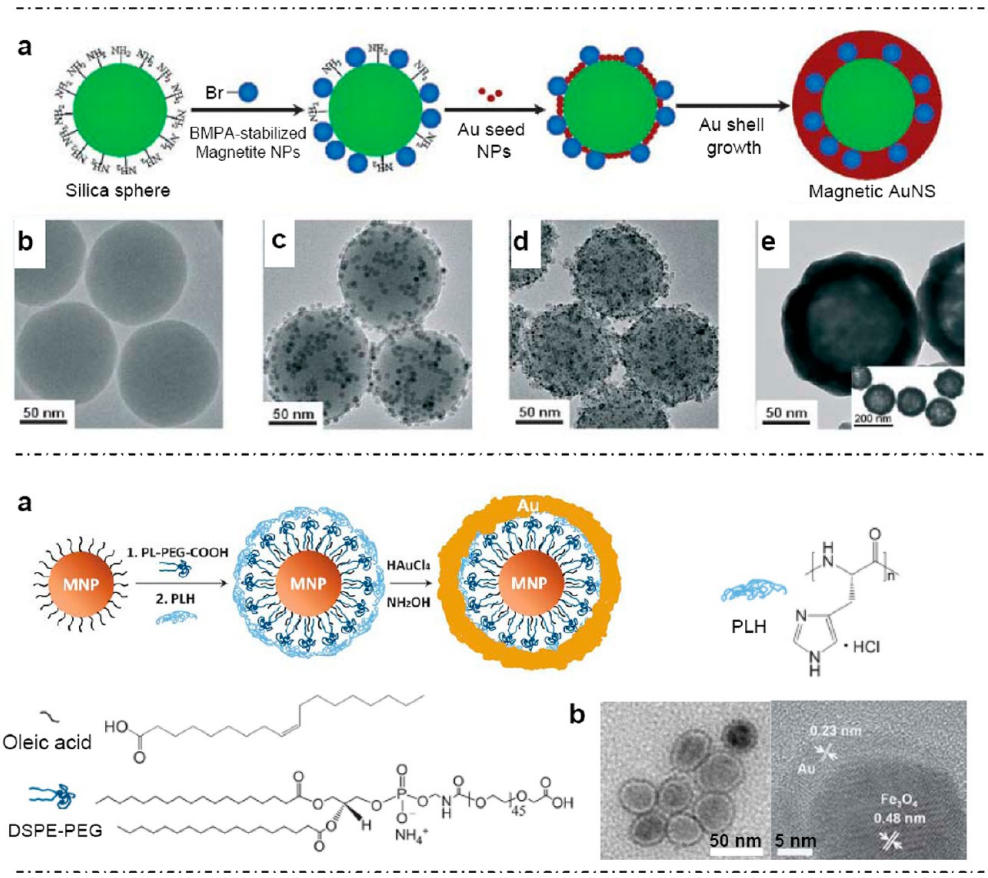

FIGURE 2. Two ways to prepare NIR-responsive Fe_3O_4–Au hybrid NPs. (Top) (a) Synthesis of the magnetic AuNSs. TEM images of (b) amino-modified silica spheres, (c) silica spheres with Fe_3O_4 NPs and (d) silica spheres with Fe_3O_4 and AuNPs immobilized on their surfaces, and (e) the magnetic AuNSs. Reprinted with permission from ref 12. Copyright 2006 Wiley-VCH. (Bottom) (a) Schematic preparation of polymer-gapped Fe_3O_4/Au core–shell NPs. Oleic acid-coated MNPs are first solubilized using amphiphilic PL-PEG-COOH. PLH is then electrostatically adsorbed onto PL-PEG-COOH for AuNS formation. The inset shows the molecular structures of oleic acid, PL-PEG-COOH and PLH. (b) Typical TEM and HRTEM images of the as-prepared Fe_3O_4/Au core–shell NPs. Reprinted with permission from ref 14. Copyright 2010 NPG.

and negatively charged because of the terminal carboxylic acids. A layer of positively charged PLH is then electrostatically adsorbed onto the outer surface of the particles at pH 5–6 for subsequent AuNS formation. The multilayer polymer coating functions as an effective barrier preventing direct growth of AuNS on the Fe_3O_4 core. Figure 2b (bottom) shows representative TEM and HRTEM images of the as-prepared Fe_3O_4/Au NPs with a 25 nm diameter Fe_3O_4 core, 2–3 nm thick AuNS, and a gap of ~3 nm between the core and shell due to the low electron density of the embedded organic molecules.

Liposome-Templated AuNS Nanocontainers. Aqueous-filled liposome (or vesicle) represents another useful "soft" core material for preparing functional core–shell NPs for biomedical applications. Compared to AuNSs that deposited on solid NPs, the liposome-templated plasmonic AuNSs can function as an ideal class of nanocontainers or carriers, which are promising for light-controlled drug/gene delivery and nanochemistry studies since cargo molecules can be encapsulated during liposome preparation and released on-demand upon irradiation at the NPs' plasmon resonant band.[15,19]

Currently there are two general formats exist for preparing cargo-loaded plasmonic vesicles. In one general format, small-sized AuNPs are combined with liposomes (e.g., by adsorbing on, forming large aggregates with, or embedding inside liposomes) loaded with cargo molecules.[15] In another format, as depicted in Figure 3a, a plasmonic vesicular nanostructure assembled from amphiphilic AuNPs with mixed polymer brush coatings.[19] The integration of AuNPs with two types of chemically distinct polymer grafts, which are analogous to block copolymers as a whole, creates a new type of hybrid building block inheriting the amphiphilicity-driven self-assembly of block copolymers to form vesicular structures and the plasmonic properties of the NPs. A key limitation, however, of such satellite AuNP-vesicle

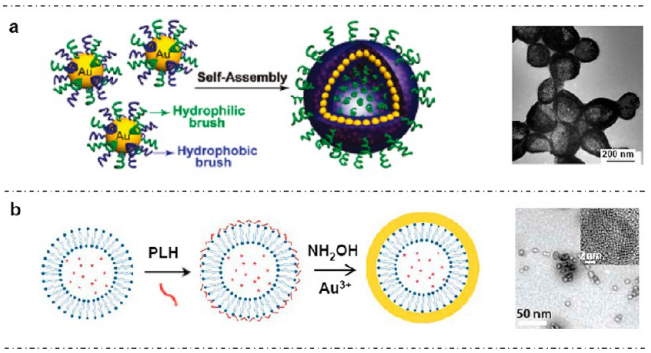

FIGURE 3. (a) Schematic illustration of self-assembly of amphiphilic nanocrystals with mixed polymer brushes into vesicular structures, and a TEM image of the plasmonic vesicles assembled from 14 nm AuNPs with mixed poly(ethyleneglycol) and poly(methyl methacrylate) brushes. Reprinted with permission from ref 19. Copyright 2011 American Chemical Society. (b) Schematic preparation of AuNS nanocontainer. Cargo-loaded liposomes are first coated with PLH monolayers for Au^{3+} immobilization. Reduction with NH_2OH leads to formation of AuNS nanocontainers. TEM and HRTEM (inset) images show small AuNS nanocontainers with mean diameters of 10 ± 3 nm. Reprinted with permission from ref 15. Copyright 2009 American Chemical Society.

assemblies is that leakage or degradation of cargo molecules is inevitable.

Aiming to create nanocontainers that are simultaneously being leakage-free in circulation (or under storage) and able to release cargo in an "on-demand" fashion, we reported a new generation of plasmonic Au nanocontainers.[15] As schematically shown in Figure 3b, cargo-loaded liposomes were first prepared by probe sonication using 1,2-dimyristoyl-*sn*-glycero-3-phosphatidic acid (DMPA) and/or 1,2-dimyristoyl-*sn*-glycero-3-phosphocholine (DMPC) as precursor lipids, followed by electrostatic deposition of PLH monolayer on their surfaces. The spatially confined AuNS growth is directed by the surface-bound PLH monolayer. In contrast to satellite AuNP-vesicle assemblies, the integrity of the nanocontainer is determined by the compact AuNS instead of the original liposome, thus rendering the nanocontainer stable and the embedded cargo unavailable at the ambient temperature. The sizes of the nanocontainers are easily tuned from 10 to 70 nm by varying the liposome size. This design has several important features that benefit for bioapplications. For example, drug/gene release can be spatially confined to targeted sites and help reduce toxicity to other cells or organs; and the release profile can be precisely controlled for optimal dosage using laser illumination at various powers.[15] The drawback of the system at the present stage lies in its difficulty in large amount preparation due to purification issues of the liposomal system, but might be addressed by combined use of, for example, a microfluidic method.[20]

Enzyme-Responsive Ag/Au Bimetallic Nanoshells. Enzyme-responsive hybrid NP systems and tactics, among the effective strategies for the synthesis and engineering of plasmonic nanostructures, have recently attracted attention because of their potential promising applications, for example, in biosensing and bioelectronics.[21,22] My group reported on an interesting enzyme-responsive plasmonic Ag/Au NS system,[23] in which control over the enzyme reaction of glucose oxidase (GOx) can automatically fine-tune the morphology and plasmonic optical response of the hybrid nanostructure. The hollow and intact Ag/Au NSs were first synthesized according to our previous method.[24,25] The citrate-stabilized Ag/Au NSs were then functionalized with a layer of PLH and enzyme GOx through electrostatic adsorption in phosphate buffer solution at pH 6–7. After purification by centrifugation to remove excess GOx, the redispersed complex Ag/Au-GOx NSs (in PBS buffer) were stored at 4 °C for subsequent experiments.[23]

Properties

Tuning LSPR of Small-Sized AuNSs to NIR Region. The LSPR responses of the silica core AuNSs can be finely tuned from visible to NIR optical window by thinning of the shell thickness (or decreasing shell thickness-to-core radius ratio) of the particle.[8] As aforementioned, conventional ways have failed to produce small-sized (<50 nm) Fe_3O_4/Au core–shell NPs with NIR responses. As shown in Figure 4a, direct coating thin layers of Au (~1 nm) onto the small Fe_3O_4 NPs (~10 nm) results in only NPs with solid AuNP-like plasmonic response in visible region (~534 nm).[18] By using our AuNS formation method and creating a few-nanometers scale polymer gap between the core and shell, we succeeded in tuning the LSPR response of the small sized (<40 nm) Fe_3O_4/Au core–shell NPs in the NIR region.[14] The polymer gap in the Fe_3O_4/Au NPs functions as an effective insulating dielectric barrier preventing gold ions from direct growth on the Fe_3O_4 core and therefore preserving the shell-type NIR response of the small NPs. Figure 4b shows the extinction spectra of the as-prepared NPs. For the case of 25 nm Fe_3O_4 core and 4–5 nm thick AuNSs, the SPR band centered around 660 nm. As the thickness decreased to 2–3 and 1–2 nm, the SPR extinction peak red-shifted to 760 and 900 nm, respectively, following a trend similar to that of silica core-AuNSs.[8]

Liposome-templated AuNSs show similar visible-NIR tunability of LSPR. Figure 4c shows extinction spectra of three liposome-templated AuNSs of ~3–4 nm shell thickness with varying size. The extinction bands of the 10, 20, and 70 nm

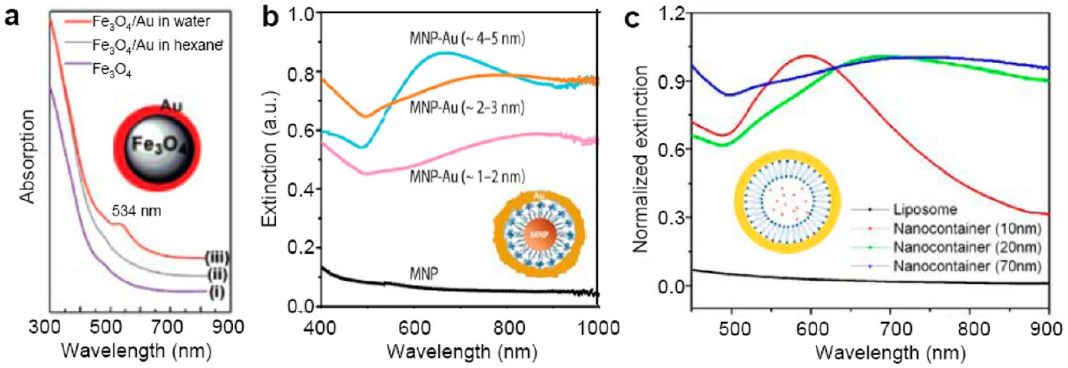

FIGURE 4. (a) UV−vis absorption spectra of the 12 nm Fe_3O_4/Au NPs prepared by direct thin Au coating in three solvants. Reprinted with permission from ref 18. Copyright 2007 American Chemical Society. (b) Extinction spectra of the polymer-coated Fe_3O_4 NPs before (black) and after formation of AuNSs of various thickness, 1−2 nm (purple), 2−3 nm (orange), and 4−5 nm (blue). Reprinted with permission from ref 14. Copyright 2010 NPG. (c) Extinction spectra of three liposome-templated AuNS nanocontainers with mean diameters of 10 ± 3, 20 ± 5, and 70 ± 10 nm, respectively. Reprinted with permission from ref 15. Copyright 2009 American Chemical Society.

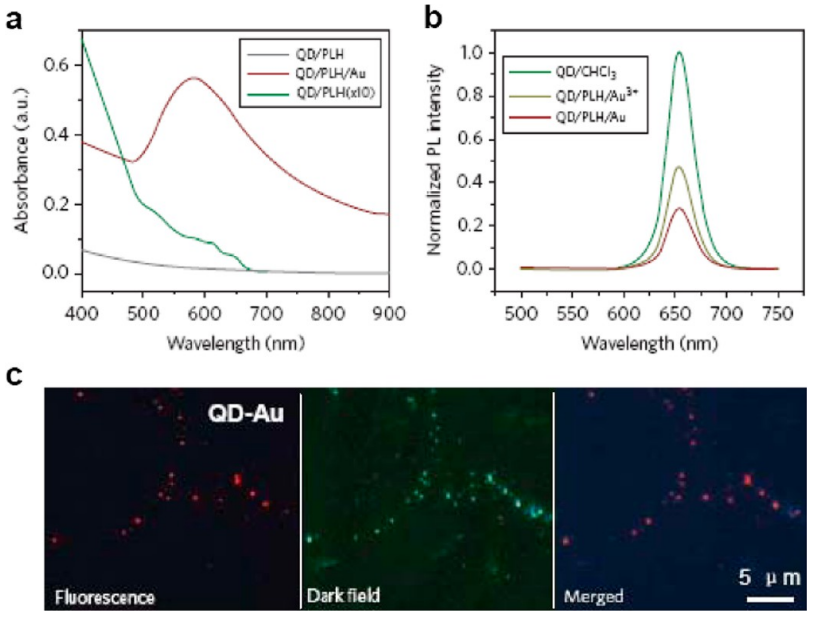

FIGURE 5. (a) UV−vis absorption spectra of the QDs before and after AuNS encapsulation. The black (original) and green (absorption value ×10 for better visualization) curves show the absorption profile of the PLH-coated QD. After AuNS formation, the QD absorption was buried by a strong SPR band centered at 583 nm. (b) Fluorescence spectra of the original organic-soluble QDs (green), water-soluble QDs in the presence of Au^{3+} ions (yellow), and Au-encapsulated QDs (red). (c) Fluorescence and dark-field imaging of single QD/Au NPs or clusters spread between two glass coverslips. Reprinted with permission from ref 13. Copyright 2009 NPG.

liposomal AuNSs are centered at ca. 600, 690, and 750 nm, respectively, with the latter two in the NIR spectral window. Compared with silica core AuNSs, the liposome-templated AuNSs exhibited poor photostability under identical laser irradiation, making them very useful for plasmonically controlled drug/gene delivery and nanochemistry studies.[15]

Multifunctionality. Due to the ultrasmall sizes of QDs (typically 3−6 nm in diameter), it is still difficult to tune LSPR of QD/Au core−shell NPs to NIR region by using our method, but the fluorescence of the QD core is effectively maintained by creating a polymer gap between the core and AuNS.[13] Therefore, the as-prepared QD/Au core−shell NPs exhibit combined fluorescent and plasmonic properties. As shown in Figure 5a, the CdSe/ZnS QDs (core) absorbed over a broad spectrum with increasing molar extinction coefficient toward shorter wavelengths and a first quantum confinement peak of 646 nm. After thin AuNS encapsulation, the QD absorption was buried under the strong Au plasmon resonance peak centered at 583 nm. Quantitative spectroscopy measurements revealed that the original organic-soluble QDs and the lipid-coated water-soluble QDs shared a similar quantum yield (QY) of 75%, whereas that of the QD/Au NPs

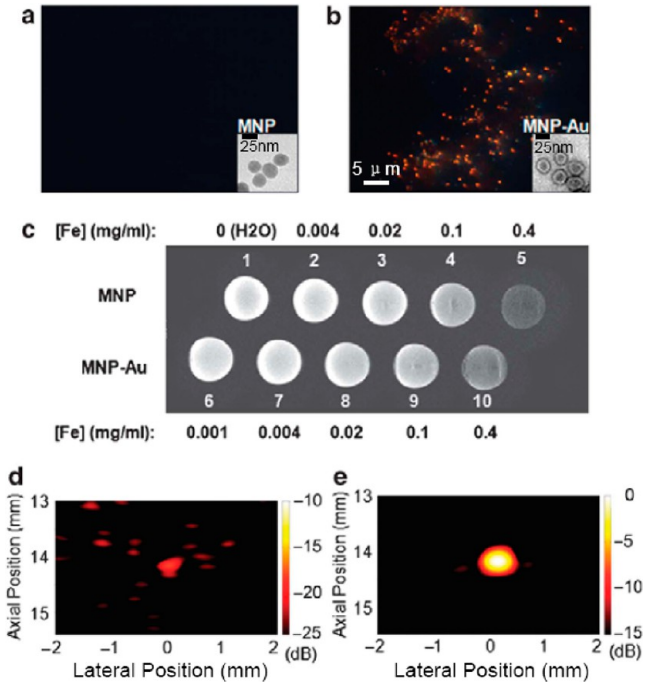

FIGURE 6. Multimodality imaging using the polymer-gaped Fe_3O_4/Au core–shell NPs. (a, b) Dark-field imaging of single Fe_3O_4 NPs spread on glass coverslips before and after AuNS coating (insets show corresponding TEM images). (c) T_2-weighted MR images of bare and Au-coated Fe_3O_4 NPs at various dilutions. Signal strength is indicated by the darkness of the images. (d, e) Cross-sectional PA images of a tube filled with (d) 5 nM Fe_3O_4 NPs and (e) 5 nM Fe_3O_4/Au NPs on a dB scale. Reprinted with permission from ref 14. Copyright 2010 NPG.

decreased to 18% (Figure 5b). The decrease in QY is thought to be mainly resulted from the interaction of plasmons and excitons in the QD/Au core–shell NPs since the magnitude of fluorescence attenuation caused by blockage of photon transmittance of the 2–3 nm thick AuNSs is much lower.[13] The fluorescence of the QD/Au NPs can be significantly improved through tuning the interaction of plasmons and excitons by increasing the core–shell separation with, for instance, successive adsorption of cationic and anionic polymers by means of layer-by-layer assembly (QY increase to ~39.0% with two bilayers of PAH/PSS);[13] and the QY could be further improved by optimizing parameters such as a broader range of core–shell spacing, shell thickness, and overlap between the QD fluorescence and Au-shell SPR bands. In addition to maintained strong fluorescence, the strong scattering property of the AuNS renders the QD/Au NPs an excellent dual-modality imaging probe. Figure 5c shows fluorescence (red) and dark-field (yellow-green colored) imaging of spatially isolated single NPs (the smallest and not-so-bright dots) or clusters (big and bright dots) of a diluted sample that spread on glass coverslips.

The polymer-gaped Fe_3O_4/Au core–shell NPs show even more highly integrated properties, including electronic, magnetic, optical, acoustic, and thermal responses, which allow multimodality imaging.[14] As compared with Fe_3O_4 NPs (Figure 6a), the strong scattering property of AuNS makes the Fe_3O_4/Au NPs an excellent optical imaging probe (Figure 6b). Since scattering-based imaging does not allow deep tissue imaging, but MRI does, we demonstrated further the MRI capability of these hybrid NPs by comparison them with conventional MNPs. Serial dilutions of MNPs with and without AuNS coating exhibited nearly identical image contrast (Figure 6c), which confirms that MNPs maintained their magnetic properties after being coated with thin AuNSs. In addition, the strong NIR absorption, and companion energy release (in the form of heat) of the AuNSs, can be used for photoacoustic (PA) imaging. To test the efficacy of the Fe_3O_4/Au NPs as PA contrast agents, water solutions consisting of no particle, 5 nM MNPs and 5 nM Fe_3O_4/Au core–shell NPs were injected sequentially into a polycarbonate tube and illuminated with a 750 nm pulsed laser. Figure 6d and e shows cross-sectional PA images of the tube corresponding to the different solutions on a decibel (dB) scale, with 0 dB corresponding to the maximum signal level across all images. Compared with the MNP solution, Fe_3O_4/Au NPs of the same concentration improved the image signal-to-noise ratio by nearly 1 order of magnitude (that is, 20 dB) because of the strong AuNS SPR absorption.

Plasmonic Applications

Biosensing. Plasmonic nanostructures are powerful platforms for ultrasensitive sensing and biosensing due to their tunable LSPR properties.[1,26] As compared with spherical solid AuNPs, AuNSs are more attractive since they offer enhanced sensitivity and functionality.[26,27] My group[23] exploited successfully the enzyme-responsive Ag/Au bimetallic NS system for innovative and sensitive nanoplasmonic glucose sensing, in which control over the enzyme reaction of surface-bound glucose oxidase (GOx) can automatically fine-tune the morphology (from compact to porous shells) and plasmonic optical response of the hybrid nanostructure. As schematically depicted in Figure 7a, the strategy is based on the selective dissolution of Ag from the preformed hollow Ag/Au bimetallic NSs by H_2O_2 which is generated from the surface-confined enzymatic oxidation of glucose in the presence of oxygen. As the enzymatic H_2O_2 etching proceeds, the LSPR band of the resultant porous NSs red-shifted gradually, reflecting the concentration change of H_2O_2, and in turn is a measure of the concentration change of

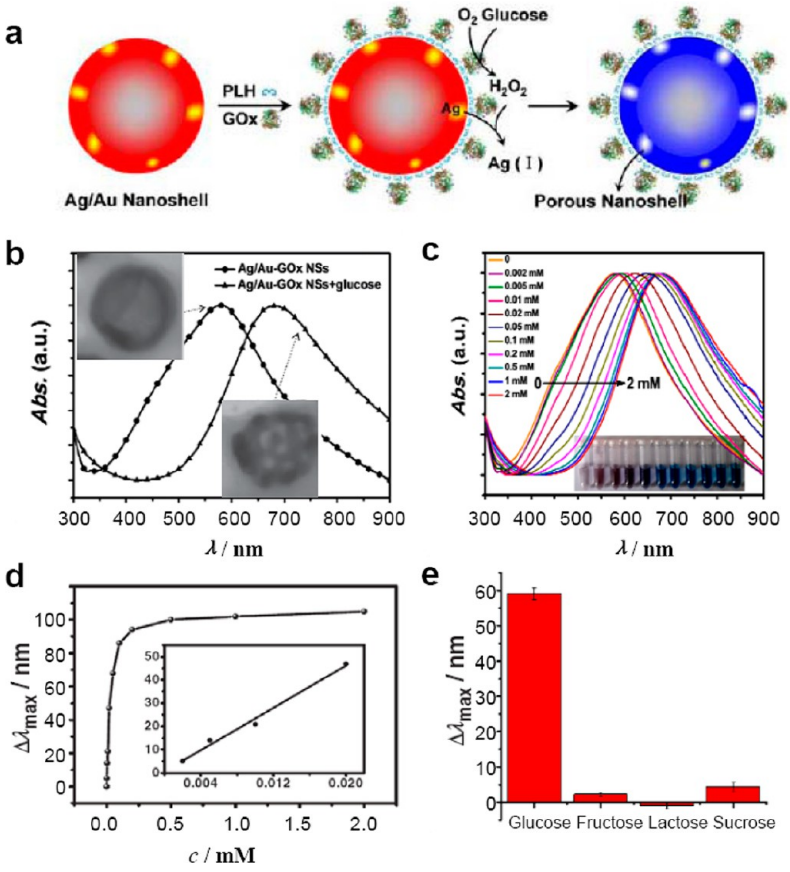

FIGURE 7. (a) Schematic preparation of hybrid Ag/Au-GOx NSs and the glucose sensing mechanism. (b) The normalized UV−vis extinction spectra and TEM images (inset) of the Ag/Au-GOx NSs before (●) and after (▲) the incubation with 2 mM glucose for 30 min. (c) The normalized UV−vis extinction spectra of the Ag/Au-GOx NSs after incubation with glucose in various concentrations for 30 min. The inset shows photograph of the corresponding reaction solutions. (d) The plot of SPR peak shift ($\Delta\lambda_{max}$) versus concentration of glucose for the Ag/Au-GOx NSs. Inset shows the linear dependence of $\Delta\lambda_{max}$ on glucose concentration. (e) Selectivity analysis for glucose detection by the SPR peak shift ($\Delta\lambda_{max}$) of UV−vis extinction spectra of the Ag/Au-GOx NSs after 30 min incubation with glucose, fructose, lactose, and sucrose. Reprinted with permission from ref 23. Copyright 2012 Wiley-VCH.

glucose in the reaction system (Figure 7). The system could detect glucose with concentrations that varied over ~1−2 orders of magnitude and down to ~0.5×10^{-3} M, and we applied this method for the detection of glucose in serum as well. We further explored the NS system for ultrasensitive in situ nanoplasmonic probing of surface-confined enzymatic activity of GOx on colloidal NPs.[28]

Magnetomotive Photoacoustic (mmPA) Imaging. Photoacoustic tomography (PAT) (or called PA imaging), an emerging technology overcomes the high degree of scattering of optical photons in biological tissue by making use of the photoacoustic effect, has been developed rapidly in the past decade and is expected to find broad applications in biology and medicine, since it can create multiscale multicontrast images of living biological structures ranging from organelles to organs.[29] As proven above, the NIR-responsive magnetic-plasmonic Fe_3O_4/Au NPs are ideal probes for scattering/MRI/PAT triple-modality imaging. And more importantly, it enables a new imaging mode, mmPA imaging, with remarkable contrast enhancement and improved specificity (by suppressing the nonmagnetomotive background) compared with PA images using conventional NP contrast agents.[14]

Due to the combination of photoacoustic effect (of AuNSs) and magnetic response (of Fe_3O_4 cores), the hybrid Fe_3O_4/Au imaging nanoprobes can be used for PAT and can erase the background noise by using a pulsing magnetic field to shake the NPs and used image processing techniques to remove everything except the vibrating pixels (Figure 8). Such background eliminating capability, together with the inexpensive, noninvasive, and high spatial resolution and deep tissue penetration nature of the PAT, make the mmPA imaging technique very sensitive and promising for clinical uses. The application and sensitivity of the imaging

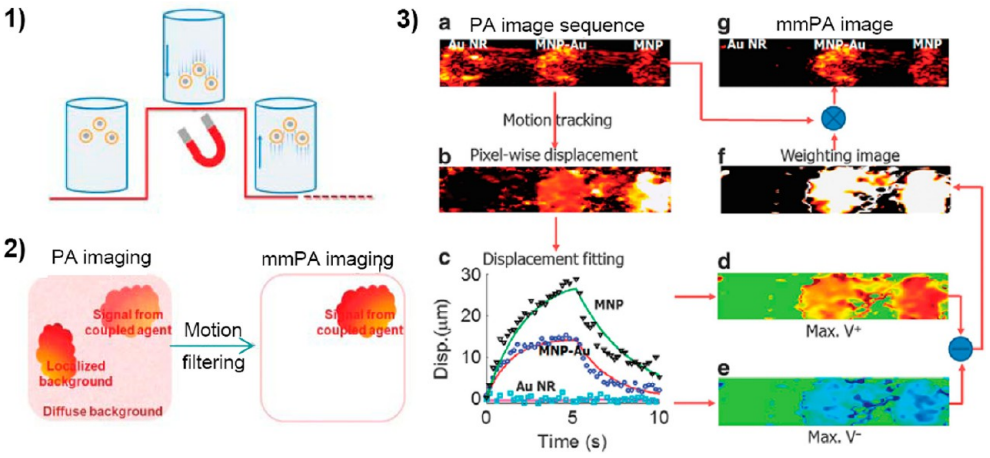

FIGURE 8. (1) Schematic of Fe_3O_4/Au core−shell NPs' response to a magnetic field. The underlying red curve represents field strength. The agents move as the magnetic field is turned on and off. (2) Schematic of contrast enhancement in mmPA imaging. mmPA imaging suppresses regions not susceptible to a controlled magnetic field while identifying regions with coupled agents responsive to a magnetic field. (3) Data processing in mmPA imaging of Fe_3O_4/Au hybrid NPs. A PVA phantom holds three 2 mm diameter inclusions, containing Au nanorods (serving as a magnetic reference and mimicking strong background tissue signals) and Fe_3O_4/Au hybrid NPs (3 nM) with comparable absorption, and MNPs (3 nM, as an optical reference), from left to right, respectively. A conventional PA image (3a) sequence acquired in synchrony with a magnetic pulse was used to acquire the maximum displacement (3b) at the end of the magnetic pulse. Three representative displacement traces and their fitted curves (3c) for pixels in different inclusions were used to compute velocity and the maximum positive and negative velocities, presented in (3d) and (3e) over a (−20, 20) μm s^{-1} display range, which were used to create a weighting image (3f) over a (0, 1) display range. mmPA image (3g) produced from the product of (3a) with (3f) over a 40 dB display range demonstrates background eliminating capability. Reprinted with permission from ref 14. Copyright 2010 NPG.

technique have been demonstrated very recently for trapping and photoacoustic detection of rare circulating tumor cells at the single cell per milliliter level with magneto-optical coupled NPs.[30] And potentially, the imaging technique can be easily combined with photothermal cancer therapy, because both techniques share similar mechanisms.[26]

Controlled Release. The liposome-templated AuNS nanocontainer represents a new generation of controlled-release vehicle that are leakage-free, spectrally programmable, and capable of light-triggered cargo release. To probe the nanocontainer stability and its cargo release capability, an organic dye (carboxyfluorescein, FAM) or anticancer drug (doxorubicin) loaded liposome was used as a model system.[15] Figure 9a and b show extinction spectra of FAM-liposomes before and after AuNS formation, and typical TEM image of small-sized AuNS nanocontainers encapsulated with FAM. Successful encapsulation of dye molecules inside the AuNS nanocontainers was confirmed by dark-field and fluorescence imaging of the same sample showing virtually complete overlap of the scattering and fluorescence signals (Figure 9c and d). Because high concentration FAM is efficiently quenched inside the nanocontainer, its fluorescence recovery after release can be used to monitor the stability and cargo release capability of the nanocontainers. As shown in Figure 9f, without laser irradiation, FAM in the parent liposomes and PLH-coated liposomes quickly leached out, indicated by the increasing fluorescence intensities, reaching their maxima in 4−5 days. In contrast, no detectable changes of fluorescence were observed for FAM in the AuNS nanocontainers after several weeks of storage.

We proceeded to investigate the nanocontainers' capability of releasing encapsulated molecules mediated by NIR light illumination. In the presence of a pulsed laser (wavelength matching AuNS's SPR wavelength), the release profile of FAM measured by its fluorescence shows a laser power-dependent behavior (Figure 9g). As the laser fluence increases (e.g., 10−20 mJ/cm^2), pronounced cargo release is revealed by the increasing fluorescence.

Advantages of the AuNSs. Compared with the silica core-AuNSs and other reported multifunctional AuNSs, the advantages of our AuNSs are obvious: they are monodisperse, compact in size (<100 nm), and highly integrated, along with tunable visible-NIR plasmonic responses, which are all crucial for in vitro or in vivo biological/biomedical studies and practical applications, especially for size and monodispersity highly dependent single cell or molecule studies. Except for controlled and traceable drug delivery, the liposome-templated AuNS nanocontainer system could also open exciting opportunities in nanochemistry.

Besides its promise for versatile bioapplications, this new class of multifunctional AuNSs, especially the plasmonic

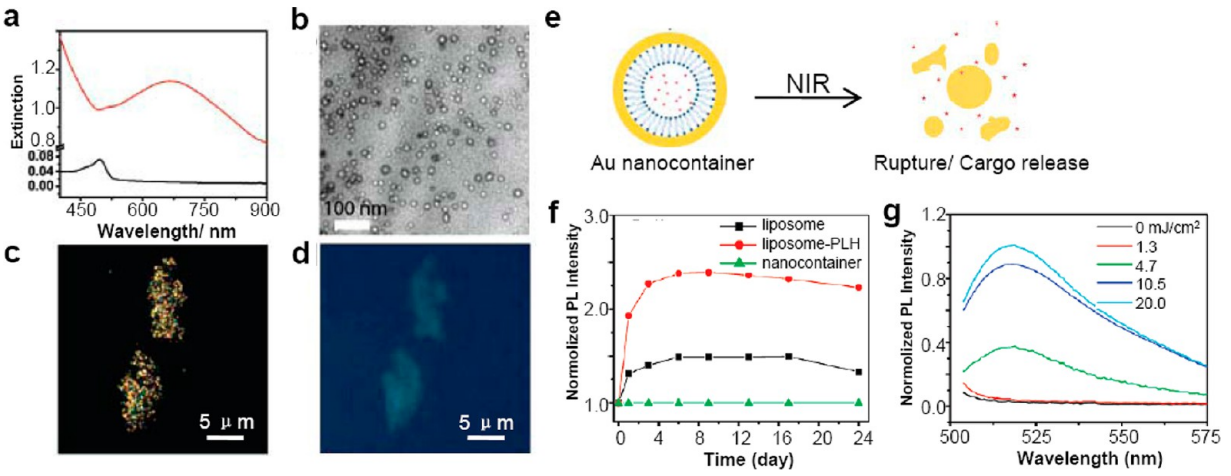

FIGURE 9. (a) Extinction spectra of FAM-liposomes before and after AuNS formation. FAM absorption centers at 495 nm (black). After AuNS formation, the extinction is dominated by the Au SPR band centered at ~680 nm (red). (b) TEM image of Au nanocontainers encapsulated with FAM. (c and d) Dark-field and fluorescence imaging of clusters of FAM-loaded Au nanocontainers, showing nearly complete overlap. (e) Schematic of NIR light-triggered deformation and cargo release of Au nanocontainer. (f) Dye release profiles of liposomes, PLH-coated liposomes, and Au nanocontainers at ambient condition and (g) Cargo release triggered by pulsed laser irradiation, measured by fluorescence intensity changes. Reprinted with permission from ref 15. Copyright 2009 American Chemical Society.

fluorescent QD/Au and magnetic plasmonic Fe_3O_4/Au core–shell NPs, due to their well-defined core–shell nanoarchitectures and underlying (nanoscale) physical interactions, may also be of fundamental importance to reveal and realize new physical phenomena and find potential useful applications.

Conclusion and Outlook

AuNSs and their nanohybrids, with tunable LSPR peaks in the NIR region, represent an important class of nanostructures and have garnered considerable attention recently for biological and cancer theranostic applications. Construction of multifunctional hybrid AuNSs compact in size with integrated functionality and maintained NIR plasmonic responses is a current pursuit in the field since such class of NSs is envisioned as a versatile and multifaceted platform for a variety of biomedical applications.

In this Account, we summarize our efforts toward the design and synthesis of multifunctional hybrid AuNSs that are compact in sizes (typically 15–60 nm), including plasmonic-fluorescent QD/Au, magnetic-plasmonic Fe_3O_4/Au core–shell NPs, liposomal AuNS nanocontainers, and enzyme-responsive Ag/Au NSs, with emphasis on the wet-chemical synthetic strategies and their unique multifunctional plasmonic properties. We have also demonstrated their innovative nanoplasmonic applications in biosensing, multimodality imaging and controlled cargo release.

One of the remaining challenges for practical in vivo applications is to produce hybrid AuNSs in large quantities (typically >0.1 g) without sacrificing the uniformity in terms of size, shape, and optical response. As such, it is necessary to scale up the production of hybrid AuNSs without compromising the quality. Due to their compact size, unique plasmonic properties and integrated multifunctionality, such hybrid AuNSs represent a next generation of AuNSs and will be gradually attracting attentions. We hope this Account has given the reader a brief sense of the great potential of such hybrid AuNSs for a diverse array of applications in biosensing, imaging and controlled release. As we and others continue to explore this promising material, it will push and lead to a "Golden Age" of plasmonic AuNPs for biomedicine.[31]

This work was supported by the Hundred Talents Program of the Chinese Academy of Sciences, the National Science Foundation of China (no. 21175125), and the State Key Laboratory of Electroanalytical Chemistry (no. 110000R387).

BIOGRAPHICAL INFORMATION

Yongdong Jin obtained his Ph.D. in Analytical Chemistry from Changchun Institute of Applied Chemistry of the Chinese Academy of Sciences in China in 2004. He did his postdoctoral work at the Weizmann Institute of Science, Israel in 2004–2006, at UCLA in 2006–2007, and at Department of Bioengineering of the University of Washington, Seattle in 2007–2010. He is presently Professor of Chemistry at the Changchun Institute of Applied Chemistry, Chinese Academy of Sciences. His present research interests include plasmonic nanostructures, bio/nanointerface and nanomedicine, energy/nano interface and catalysis, and nanopore-based analytics.

FOOTNOTES

*E-mail: ydjin@ciac.ac.cn.
The authors declare no competing financial interest.

REFERENCES

1 Anker, J. N.; Hall, W. P.; Lyandres, O.; Shan, N. C.; Zhao, J.; Van Duyne, R. P. Biosensing with plasmonic nanosensors. *Nat. Mater.* **2008**, *7*, 442–453.

2 Wax, A.; Sokolov, K. Molecular imaging and darkfield microspectroscopy of live cells using gold plasmonic nanoparticles. *Laser Photonics Rev.* **2009**, *3*, 146–158.

3 Li, Y.; Jing, C.; Zhang, L.; Long, Y.-T. Resonance scattering particles as biological nanosensors in vitro and in vivo. *Chem. Soc. Rev.* **2012**, *41*, 632–642.

4 Cobley, C. M.; Chen, J. Y.; Cho, E. C.; Wang, L. V.; Xia, Y. N. Gold nanostructures: a class of multifunctional materials for biomedical applications. *Chem. Soc. Rev.* **2011**, *40*, 44–56.

5 Ozbay, E. Plasmonics: Merging photonics and electronics at nanoscale dimensions. *Science* **2006**, *311*, 189–193.

6 Atwater, H. A.; Polman, A. Plasmonics for improved photovoltaic devices. *Nat. Mater.* **2010**, *9*, 205–213.

7 Bardhan, R.; LaL, S.; Joshi, A.; Halas, N. J. Theranostic nanoshells: from probe design to imaging and treatment of cancer. *Acc. Chem. Res.* **2011**, *44*, 936–946 and references therein.

8 Oldenburg, S. J.; Averitt, R. D.; Westcott, S. L.; Halas, N. J. Nanoengineering of optical resonances. *Chem. Phys. Lett.* **1998**, *288*, 243–247.

9 Louie, A. Y. Multimodality imaging probes: design and challenges. *Chem. Rev.* **2010**, *110*, 3146–3195.

10 Dreher, M. R.; Liu, W. G.; Michelich, C. R.; Dewhirst, M. W.; Yuan, F.; Chilkoti, A. Tumor vascular permeability, accumulation, and penetration of macromolecular drug carriers. *J. Natl. Cancer Inst.* **2006**, *98*, 335–344.

11 Choi, H. S.; Liu, W.; Misra, P.; Tanaka, E.; Zimmer, J. P.; Ipe, B. I.; Bawendi, M. G.; Frangioni, J. Renal clearance of quantum dots. *Nat. Biotechnol.* **2007**, *25*, 1165–1170.

12 Kim, J.; Park, S.; Lee, J. E.; Jin, S. M.; Lee, L. J. H.; Lee, I. S.; Yang, I.; Kim, J.-S.; Kim, S. K.; Cho, M.-H.; Hyeon, T. Designed fabrication of multifunctional magnetic gold nanoshells and their application to magnetic resonance imaging and photothermal therapy. *Angew. Chem., Int. Ed.* **2006**, *45*, 7754–7758.

13 Jin, Y. D.; Gao, X. H. Plasmonic fluorescent quantum dots. *Nat. Nanotechnol.* **2009**, *4*, 571–576.

14 Jin, Y. D.; Jia, C. X.; Huang, S.-W.; O'Donnell, M.; Gao, X. H. Multifunctional nanoparticles as coupled contrast agents. *Nat. Commun.* **2010**, *1*, 41 and references therein.

15 Jin, Y. D.; Gao, X. H. Spectrally tunable leakage-free gold nanocontainers. *J. Am. Chem. Soc.* **2009**, *131*, 17774–17776 and references therein.

16 Bruchez, M.; Moronne, M.; Gin, P.; Weiss, S.; Alivisatos, A. P. Semiconductor nanocrystals as fluorescent biological labels. *Science* **1998**, *281*, 2013–2016.

17 Lyon, J. L.; Fleming, D. A.; Stone, M. B.; Schiffer, P.; Williams, M. E. Synthesis of Fe oxide core/Au shell nanoparticles by iterative hydroxylamine seeding. *Nano Lett.* **2004**, *4*, 719–723.

18 Xu, Z. C.; Hou, Y. L.; Sun, S. H. Magnetic core/shell Fe_3O_4/Au and Fe_3O_4/Au/Ag nanoparticles with tunable plasmonic properties. *J. Am. Chem. Soc.* **2007**, *129*, 8698–8699.

19 Song, J. B.; Cheng, L.; Liu, A. P.; Yin, J.; Kuang, M.; Duan, H. W. Plasmonic vesicles of amphiphilic gold nanocrystals: self-assembly and external-stimuli-triggered destruction. *J. Am. Chem. Soc.* **2011**, *133*, 10760–10763.

20 Duraiswamy, S.; Khan, S. A. Plasmonic nanoshell synthesis in microfluidic composite foams. *Nano Lett.* **2010**, *10*, 3757–3763.

21 Willner, I.; Baron, R.; Willner, B. Integrated nanoparticle-biomolecule systems for biosensing and bioelectronics. *Biosens. Bioelectron.* **2007**, *22*, 1841–1852.

22 Zhang, L.; Li, Y.; Li, D.-W.; Jing, C.; Chen, X. Y.; Lv, M.; Huang, Q.; Long, Y.-T.; Willner, I. Single gold nanoparticles as real-time optical probes for the detection of NADH-dependent intracellular metabolic enzymatic pathways. *Angew. Chem., Int. Ed.* **2011**, *50*, 6789–6792.

23 He, H. L.; Xu, X. L.; Wu, H. X.; Jin, Y. D. Enzymatic plasmonic engineering of Ag/Au bimetallic nanoshells and their use for sensitive optical glucose sensing. *Adv. Mater.* **2012**, *24*, 1736–1740.

24 Jin, Y. D.; Dong, S. J. Diffusion-limited, aggregation-based, mesoscopic assembly of roughened core shell bimetallic nanoparticles into fractal networks at the air-water interface. *Angew. Chem., Int. Ed.* **2002**, *41*, 1040–1044.

25 Wu, H. X.; Wang, P.; He, H. L.; Jin, Y. D. Controlled synthesis of porous Ag/Au bimetallic hollow nanoshells with tunable plasmonic and catalytic properties. *Nano Res.* **2012**, *5*, 135–144.

26 Jin, Y. D. Engineering plasmonic gold nanostructures and metamaterials for biosensing and nanomedicine. *Adv. Mater.* **2012**, *24*, 5153–5165.

27 Raschke, G.; Brogl, S.; Susha, A. S.; Rogach, A. L.; Klar, T. A.; Feldmann, J. Gold nanoshells improve single nanoparticle molecular sensors. *Nano Lett.* **2004**, *4*, 1853–1857.

28 He, H. L.; Xu, X. L.; Wu, H. X.; Zhai, Y. J.; Jin, Y. D. In situ nanoplasmonic probing of enzymatic activity of monolayer-confined glucose oxidase on colloidal nanoparticles. *Anal. Chem.* **2013**, *85*, 4546–4553.

29 Wang, L. V.; Hu, S. Photoacoustic tomography: in vivo imaging from organelles to organs. *Science* **2012**, *335*, 1458–1462.

30 Hu, X. G.; Wei, C.-W.; Xia, J. J.; Pelivanov, I.; O'Donnell, M.; Gao, X. H. Trapping and photoacoustic detection of CTCs at the single cell per milliliter level with magneto-optical coupled nanoparticles. *Small* **2013**, *9*, 2046–2052.

31 Dreaden, E. C.; Alkilany, A. M.; Huang, X. H.; Murphy, C. J.; El-Sayed, M. A. The golden age: gold nanoparticles for biomedicine. *Chem. Soc. Rev.* **2012**, *41*, 2740–2779.